Electronic Supplementary Material (ESI) for Materials Advances.

SUPPORTING INFORMATION

Efficient and Highly Biocompatible 8-arm PEG-Chlorin e6 Nanosystems for 2-Photon Photodynamic Therapy of Adrenergic Disorders

Natalie S. Potter,† Zhen Wang, ‡ Evan C. Bornowski, † Scott D. Swanson,¶ John P. Wolfe, † Alan McLean*,† and Raoul Kopelman†

† Department of Chemistry, University of Michigan 930 N. University Ave., Ann Arbor, MI 48109, United States

‡ Melville Laboratory for Polymer Synthesis, Yusuf Hamied Department of Chemistry, University of Cambridge, Lensfield Road, Cambridge CB2 1EW, UK

¶ Department of Radiology, University of Michigan, 1500 East Medical Center Dr., Ann Arbor, MI 48105, United States

E-mail: ammclean@umich.edu

Table of contents

SECTION S1 – EXPERIMENTAL PROCEDURES

General Information

8-arm PEG-NH_2 (40 kDa) and maleimide-PEG-SCM (2 kDa) were purchased from CreativePEGWorks (Chapel Hill, NC). Chlorin e6 was purchased from Frontier Scientific. All other chemicals were bought from Sigma-Aldrich (St. Louis, MO) or Thermo Fischer Scientific (Grand Island, NY) of the best grade possible and no additional purification was done. Nitrogen was used to obtain any anhydrous solvent from Sure/Seal™ bottles and was used for any reactions run under inert air. Argon was used for large volume washes with an Amicon™ Stirred Cell, fitted with a 10kDa filter. A Thermoscientific Sorvall ST 16R Centrifuge was used with a 10 kDa MilliporeSigma™ Amicon™ Ultra-2 Centrifugal Filter Units for smaller volume washes. Millipore water was dispensed from a Synergy® UV System and lyophilization was done using a Labonco Freezone 4.5.

Synthesis of MIBG-3-MPAM and BG-3-MPAM

MIBG-3-MPAM was synthesized in 6 synthetic steps and BG-3-MPAM was synthesized in 4 steps both following our previous protocol.[1] All intermediate steps were purified with flash chromatography except for formation of the final product. NMR and MS characterizations were used to verify the formation each intermediate and final products.

MIBG-3-MPAM:

H^1 NMR: 9.51 (s, 1H, NH), 8.02 (t, 1H, ArH), 7.77 (s, 1H, NH), 7.35 (d, 1H, ArH), 7.25 (d, 1H, ArH), 4.31 (d, 2H, C**H**$_2$N), 2.71 (t, 2H, CH_2), 2.62(t, 2H, CH_2), 2.47(s, 2H, NH_2), 1.26(s, 1H, SH). MS m/z: 379.0084.

BG-3-MPAM:

H^1 NMR: 11.64 (s, 2H, NH_2), 10.02 (s, 1H, NH), 7.97 (s, 1H, NH), 7.60 (d, 2H, ArH), 7.24 (d, 2H, ArH), 4.30 (d, 2H, CH_2N), 2.73 (t, 2H, CH_2), 2.63 (t, 2H, CH_2), 1.26(s, 1H, SH). MS m/z: 253.1118

Synthesis of 8-arm PEG-Ce6

Ce6 was conjugated to 8-arm PEG via DCC/NHS coupling in DMF. For 30 min 22.38 mg of Ce6 solution (3 equiv., 20 mg/mL in DMF) was mixed with 387 µL of N,N'-dicyclohexylcarbodiimide (DCC) (3 equiv., 20 mg/mL in DMF) and 431.6 µL of N-hydroxy succinimide (NHS) (6 equiv., 20 mg/mL in DMF). 500 mg of 8-arm PEG (40kDa) was solvated in DMF (50 mg/mL). To ensure full solvation a vortex mixer was utilized. The Ce6 solution was added to the 8-arm PEG solution and allowed to stir overnight. Following the overnight reaction, unconjugated Ce6 was removed using a 50:50 mixture of ethanol/PBS in an Amicon Cell filtration system using a 10 kDa filter membrane. This was repeated until the solution runs clear. Once wash solution is clear, the solvent was exchanged with Millipore ultrapure water and let run 2x. Resulting material was filtered using a 0.45 µm syringe filter and freeze-dried for storage and UV-vis was used for conjugation verification.

Conjugation of dMIBG/dMBG to 8-arm PEG-Ce6

The conjugation of the small molecules ('MIBG-3-MPAM and 'BG-3-MPAM') follows a modified protocol from previous literature.[2] 66mg of heterobifunctional malemide PEG-NHS (MAL-PEG-NHS, 2kDa, Creative PEG works)(100mg/mL in 10X PBS) is added to 33mg of 8-arm-PEG-ce6 (20mg/mL in 10X PBS) and stirred for one hour. Unreacted MAL-PEG-NHS was washed out with 10X PBS using an 10kDa Amicon centrifugal cell two times. To wash out remaining PBS, the sample was washed

twice with MilliQ water. The remaining sample was re-suspend in MeOH (20mg/mL). 40x molar equivalence of dMIBG or dMBG (dissolved in minimal MeOH) was added and the reaction was let stir for two hours. The reaction was diluted in 10X PBS to <60%MeOH before adding to Amicon cell. After the initial filtration, the sample was washed two more times with MilliQ water. 10X PBS was used to resuspend the reaction and immediately 40x molar equivalence of cysteine (20mg/mL in 10X PBS, pH 7.4) was added and let stir for 15 minutes. Using a 10kDa Amicon cell the sample was washed three times with 10X PBS. Lastly, the final product was washed three times with MilliQ water.

UV-Vis absorption

UV-Vis absorption was measured using a Shimadzu UV-1601. Samples (Rose Bengal, TMPyP, Ce6, 8-arm PEG-Ce6, and 8-arm PEG-Ce6-dMIBG/dBG) were prepared in 1 mL or 4 mL disposable plastic cuvettes in a 1X PBS solution for ROS efficacy experiments. For calculating the Ce6 conjugation ratio, the lambda max at 660 nm was used for calibration as spectral overlap of the Ce6 *Soret* band and the 8-arm PEG around 400 nm prevents the 1-photon 400 nm peak (equivalent to the 2-photon 800 nm excitation wavelength) from being used for this calculation.[3] For 2-photon cross-section measurements, Coumarin 307 was prepared in methanol (MeOH) and Coumarin 153 was prepared in ethanol (EtOH) for quantum yield measurements.

Transmission Electron Microscopy (TEM)

Transmission electron microscopy was performed using a JEOL JEM 1400 electron microscope at 60 kV under vacuum. For imaging, 8-arm PEG-Ce6-dMIBG NPs at 0.1, 0.5 and 1.0 mg/mL were drop-deposited onto a carbon-coated Formvar film grid

('Carbon Type B' TED Pella #01810) and dried. It should be noted that the presence of iodine allowed the NPs to be visualized in a standard TEM mode with good experimental contrast (dark circles), allowing for quantitative nanoparticle size analysis (uranyl acetate staining not required). The MIBG-3-MPAM, BG-3-MPAM, and non-targeted 8-arm PEG-Ce6 were all stained with uranyl acetate post-sample deposition (1% solution for 5 min), but the TEM imaging resolution was substantially decreased, therefore the 8-arm-PEG-dMIBG images were used to determine the NP size (the dMIBG/dBG ligand does not substantially affect the NP size, therefore the NP diameter would be approximately equivalent across all samples). The 8-arm PEG-Ce6-dMIBG NP TEM size analysis was performed in ImageJ. TEM images were first rolling ball corrected (radius = 50.0 pixels, light pixels selected) over 2 iterations to smooth the background. After that, the white intensity threshold was adjusted to an approximate 5% lower limit, to select features and remove artificial features. Particles were subsequently analyzed utilizing particle area thresholds (nm^2) from 20 (minimum area) to infinity (maximum area). Minimum area was selected at 20 nm^2 (approx. 3 nm diameter), to avoid capturing noise speckle, and circularity was selected between 0.75-1.00.

Diffusion Ordered NMR Spectroscopy + Quantitative NMR Analysis + Size analysis

Diffusion-order NMR spectra were recorded at an ambient temperature probe, using a Varian Vnmr 700MHz spectrometer. The chemical shifts are reported as ppm and the solvent residual peak is marked for DMSO-d_6 (2.50 ppm and 3.33 ppm due to water) and D_2O (4.8 ppm). The parameters of the DOSY method increased the gradient value from 1300 G/cm to a highest gradient value of 32500 G/cm in 15 increments.

Diffusion gradient length was set to 4.0 ms with a 100 ms diffusion delay and a 1 s relaxation delay.

Previously, it was shown that the translational diffusion coefficient of the 8-arm PEG nanosystem was about 2 orders of magnitude larger than that of the water molecule, which allows the isolation of the 8-arm PEG from its water environment by suppressing the water peak around 3.33 ppm through a pulsed gradient diffusion experiment and allows for quantitative NMR analysis and size analysis.[4] For the quantitative NMR analysis, characteristic peaks were identified and integrated. The molar ratios were then calculated using this reported method. Using equation (1) the molar ratio of the targeting molecules (dMIBG and dBG) to that of Ce6 was calculated,

$$\frac{M_x}{M_y} = \frac{I_x}{I_y} * \frac{N_y}{N_x} \qquad (1)$$

where M_x/M_y is the molar ratio, I_x and I_y are the integrations, and N_y and N_x are the number of expected nuclei.[5] The molar ratio of dMIBG and dBG to 8-arm PEG was then calculated using the known ratio of Ce6 to 8-arm PEG (2.01 to 1).

For the size analysis, the diffusional coefficient (D_T) was estimated by performing a DOSY process through the Vnmrj software which fits the peak intensity decay due to a pair of pulsed magnetic field gradients in a stimulated echo experiment to

$$\mathrm{I} = \mathrm{I}_0 \mathrm{e}^{-\mathrm{D_T Z}} \qquad (2)$$

$$\text{Where } \mathrm{Z} = \gamma^2 \mathrm{G}^2 \delta^2 \left(\Delta - \frac{\delta}{3}\right),$$

γ is the proton gyromagnetic ratio, G is the amplitude of the applied gradient, δ is the duration of the applied gradient, and Δ is the separation time between gradient pairs.[6] Once D_T was calculated, it was used in the following Stokes-Einstein equation (3) to

determine the hydrodynamic radius (R_H) and subsequentially the hydrodynamic diameter or size reported in the main manuscript.[7]

$$D_T = \frac{k_B T}{6\pi\eta R_H} \qquad (3)$$

Where T is the temperature, k_B is the Boltzmann constant, and η is the dynamic viscosity.

Gel Permeation Chromatography

Gel permeation chromatography (GPC) for the 8-arm PEG-Ce6, 8-arm PEG-Ce6-dMIBG, and 8-arm PEG-Ce6-dBG samples was performed on a Shimadzu HPLC system composed of a CBM-20A control unit, an LC-20AD Pump, an SIL-20A autosampler, and a CTO-20A column oven. An aqueous solution including sodium nitrate (0.1 M) and sodium azide (0.01 M) was used as the eluent, at a flow rate of 1.0 mL/min. The column set consists of 1 × PSS SUPREMA precolumn (8 × 50 mm), 1 × PSS SUPREMA S4 analytical 100 Å (8 × 300 mm), and 2 × PSS SUPREMA analytical 3000 Å (8 × 300 mm). The GPC was connected in series with a UV-Vis photodiode array detector (for optically active samples that include Ce6), a Wyatt DAWN HELEOS-II multiangle light scattering (MALS) detector (laser at λ = 658 nm), and a Wyatt Optilab rEX differential refractive index (DRI) detector (λ = 658 nm light source). The column temperature and the detector temperature were controlled at 30 °C. All data analysis was done using Wyatt Astra V 6.1 software. The concentration for samples was tested between 5.0 mg/mL and 0.5 mg/mL. A literature value for the d*n*/d*c* of poly(ethylene glycol) in water of 0.134 mL/g was used to determine the PEG molecular weight.[8]

For the MAL-PEG-SCM sample, GPC was performed on a Shimadzu GPC fitted with a non-aqueous phenogel 10μm Linear (2) LC column. The mobile phase was THF.

The GPC was connected to a refractive index detector and a diode array UV-Vis detector. The RID is a Shimadzu-10A set to positive polarity (no wavelength is reported or controlled). The column temperature was held at 40 °C and a flow rate of 1 mL/min was used. All data extraction was done using the Shimadzu LC Solutions software., which is calibrated against toluene and narrow mass range polystyrene standards ranging from 1050 Da to 1Mda.

Fluorescence Quantum Yield

The fluorescence quantum yield of Ce6, 8-arm PEG-Ce6, 8-arm PEG-Ce6-dMIBG and dBG were measured following a previous protocol.[9] These measurements were done using a Horiba PTI QuantaMaster Fluorimeter. Samples were prepared in 1X PBS and matched to an OD of 0.1, at 400 nm. Coumarin 153, with a known fluorescence quantum yield of 0.54, was used as the standard and was prepared in EtOH and matched to the same 0.1 OD at 400 nm.[10] All samples were excited at 400 nm and the emission spectra were taken from 410-900 nm. To analyze the data, the areas under the peaks were calculated and used in the following equation (4)[10]:

$$\Phi_{\mathrm{f}}^{i} = \frac{F^{i} f_{s} n_{i}^{2}}{F^{s} f_{i} n_{s}^{2}} \Phi_{\mathrm{f}}^{s} \quad (4)$$

$$Where\ f_x = 1 - 10^{-Ax}$$

Here A is the absorbance, i is the sample, F is the integrated intensity (area under fluorescence curve), f is the absorption factors (see above equation), *s* is the standard, and n is the refractive index. The integrated intensity was done using the integration function in OriginLab.

ROS Efficacy

The ROS efficacy was measured using the following indirect sensing probe method. Singlet Oxygen Sensor Green (SOSG) was used as the fluorescent indicator since SOSG in the presence of $^1O_2$ is converted into SOSG-EP, which shows a fluorescent emission at 530 nm, when excited at 504 nm.[11] The fluorescence intensity of SOSG-EP increases with the increase in $^1O_2$ production. Samples dissolved in 1X PBS were matched to an O.D. of 0.1 at 400 nm, for 5,10,15,20-tetrakis(1-methyl-4-pyridinio)porphyrin tetra(p-toluene-sulfonate) (TMPyP), Ce6, 8-arm PEG-Ce6, 8-arm PEG-Ce6-dMIBG/dBG and at 549 nm for Rose Bengal (RB). For the preparation of SOSG, 500 µL of MeOH was added to one 100 µg vial for a final concentration of ~0.3mM. 40 µL of SOSG (~0.3mM in MeOH) was added to 1 mL of dye solution or nanoparticles solution for a final SOSG concentration of 12 µM. The mixtures were then allowed to stir, covered for 5 min before use. The emission spectrum of SOSG-EP was measured using an emission wavelength of 504 nm and an excitation range of 520-600 nm, with an integration time of 0.1000s and a slit size of 2 nm. All samples were excited at 100 s intervals (at 549 nm for RB and 400 nm for all other samples) and then allowed to sit unchanged for 3 minutes before the fluorescence emission of SOSG-EP was measured again, using a Horiba PTI QuantaMaster Fluorometer.

To calculate the singlet oxygen efficacy, RB was used as the standard with a known efficacy of 0.75.[11] Equation (4) was employed using the relationship between the slopes of the SOSG-EP intensity at 530 nm vs. total irradiation time and the known RB efficacy.[12]

$$\phi_\Delta = \phi_\Delta^{std} \frac{k_{SOSG} I_{abs}^{std}}{k_{SOSG}^{std} I_{abs}} \qquad (5)$$

Here the *k* are the first order rate constants (slopes from the SOSG-EP vs. time graph), the *I* are the absorption values, and ϕ indicates the singlet oxygen quantum yield/efficacy. Since the sample absorptions are matched at 0.1, for our experiment we can assume that $\frac{I_{abs}^{std}}{I_{abs}} = 1$.

2-Photon Cross-Section

The TPEF method was utilized to measure the 2-photon cross-section of Ce6 and of the 8-arm PEG-Ce6 nanosystems, using the following method.[13] A mode-locked 100 fs pulsed TI:Sapphire laser, with a repetition rate of 80 MHz, was focused on the sample. An 800 nm excitation was used, and the fluorescence was collected by an Action Instrument SpectraPro 3000 with a Hammatsu 928 PMT set at 800 V. To control the input power, a neutral density filter was applied. Coumarin 307 in MeOH was used as a reference with a known cross-section at 800 nm ($\delta\eta_{800} = 14.7\ GM$).

To calculate the 2-photon cross-section from the fluorescence of a given molecule, the following equation (6) from Xu et al. was applied:[14]

$$\log[F(t)] = 2\log[P(t)] + \log\left[\frac{1}{2}\eta\phi\delta[c]\frac{g_p}{f\tau}\frac{8n}{\pi\lambda}\right] \qquad (6)$$

Where *F(t)* is the 2-photon fluorescence, *P(t)* is the excitation power, *n* is the refractive index of the solvent, *[c]* is the concentration of the molecule, η is the quantum yield of the molecule, ϕ is the collection efficiency, δ is the 2-photon cross section of the molecule, λ is the laser wavelength, g_p is the "second-order temporal coherence", f is the pulse repetition rate, and τ is the excitation pulse width (FWHM) – together $f\tau$ is the "duty cycle".

Equation (6) is written in the y = mx + b form and applied to the TPEF method through a ratiometric comparison between a known reference 2-photon dye and the sample of interest. The 2-photon cross-section is then calculated using equation (7), where δ is the 2-photon cross section, b is the y-intercept of the log(fluorescence)-log (power) plot, η is the quantum yield, n is the refractive index, and *[c]* is the concentration:

$$\eta_{sample}\delta_{sample} = \frac{10^{b_{sample}-b_{std}}\eta_{std}\delta_{std}\,[c]_{std}n_{std}}{[c]_{sample}n_{sample}} \qquad (7)$$

Cell Culture

SK-N-BE(2)C cells were grown in DMEM culture medium containing 1% penicillin/streptomycin and 10% fetal bovine serum. Cells were split every 3-4 days or until confluency of 70-80% was reached. The cells were incubated at 37 ºC in a 5% CO_2 environment.

Cell Viability – MTT Assay

3-(4,5-dimethylthiazol-2-yl)-2,5-diphenyltetrazolium bromide (MTT) was used to determine the cell viability of SK-N-BE(2)C neuroblastoma cells after a 24 hr exposure to the 8-arm PEG-Ce6-dMIBG. 5,000 cells were plated onto a 96 well plate in 100 µL of DMEM media and were incubated. After 24 hrs, the 8-arm PEG-Ce6-dMIBG in 1X PBS was added, at 0.5, 2, 10, 100, 500, 1000 molar equivalence to Ce6, to 6 wells. The wells were brought up to 200 µL using additional media. No nanoparticle was added to the control row. A solution of MTT dye in 1X PBS (5.0 mg/mL) was filtered, using a 0.22 µm pore size, to sterilize and to remove any insoluble residue. 20 µL of the filtered MTT dye was added to all wells, for a final concentration of 0.45 mg/mL. The cells were

allowed to incubate for 3 hrs at 37 C. The media was aspirated and 200 µL of DMSO was added to each well, to dissolve all the crystals. Note that a row of pure DMSO was included as a blank reference. After another hour of incubation, to ensure all crystals were dissolved, the plate was read on an Anthos 2010 plate reader and scanned, using a measurement filter at 550 nm and a reference wavelength of 620 nm.

2-Photon Photodynamic Therapy and Imaging

SK-N-Be(2)c cells were plated onto grided petri dishes at 300,000 cells/plate a day before the experiment. 2 hours before imaging, noncontrol plates were incubated with 8-arm PEG-Ce6, 8-arm PEG-Ce6-dMIBG, and 8-arm PEG-Ce6-dMBG at 1uM equiv. of Ce6 – UV-vis used to verify the concentration equivalence. 1.5 hours after the nanoparticles were added, a 2.5µL/1mL aliquot of Calcein AM (50µg/50µl in DMSO) was added to the plates. After a 30 min incubation, the plate was washed three times with DPBS media. Next, 1mL of colorless DMEM media was added to the plate and 20µL of propidium iodide (PI) at 1mg/mL (in PBS) was added.

A Leica SP8 Inverted confocal microscope with a coupled Ti:Sapphire laser for multiphoton excitation with a 100 femtosecond pulse width and a 80 MHz repetition rate was used for both 2-photon photodynamic therapy excitation and confocal fluorescence imaging of cell labels (before and after PDT). SK-N-Be(2)C cells were 2-photon excited at 2.4mW power for 10 scans (400 Hz speed, 1.2 µm pixel dwell-time) using a 40x water objective within a 250 µm x 250 µm box. These chosen parameters were inspired by the work of Ventura and co.[15,16] Confocal fluorescence images were acquired using a 10x dry objective and Calcein AM (green-colorized) and propidium iodide (red-colorized) filters in the emission ranges of 498 – 540 nm and 569 – 611 nm using separate

detectors with a white light excitation source. Images were taken before and 12 hours after excitation.

Imaging Analysis

To quantify the efficacy of the 2-photon photodynamic therapy experiments, we used FIJI (ImageJ) to analyze the propidium iodide fluorescence before and after photodynamic therapy excitation. We analyzed PI fluorescence for two reasons: 1.) Calcein AM, while serving as a marker for viable cells, is known to slowly leak out of cells over time,[17] 2.) Propidium iodide (PI) is a well-known marker for dead cells.[18]

.LIF images were imported directly into FIJI (the BioImporter plugin is required) to preserve the separation between calcein AM and propidium iodide channels. For all samples, a 775.76 μm x 775.76 μm area was used. To quantify fluorescence noise, 3-4 images of each region were imported, noise was approximately 46% for PI (initial) and 14% for calcein (initial). In order to quantitate the photodynamic therapy effect, an average propidium iodide background before PDT was first determined by measuring (*FIJI, Analyze, Measure)* the propidium iodide fluorescence (integrated intensity) in FIJI before excitation across trials. To standardize the cell density across samples, the propidium iodide signal (counts) before PDT was divided by the measured calcein AM signal (counts), as nearly all cells begin healthy, with intense calcein fluorescence approximately proportional to number of cells in the area. Next, we determined the final propidium iodide signal (counts) 12 hours after PDT for each sample, which was density-standardized by Calcein AM. These two operations can be summarized as,

$$Avg.PI\ background_{before\ PDT} = \sum \frac{\frac{PI\ fluorescence\ (counts)_{intial}}{Calcein\ AM\ fluorescence\ (counts)_{initial}}}{n} \quad (8)$$

where *n* is the number of trials (for both trial 1 and trial 2, *n* = 4),

and,

$$PI\ signal_{after\ PDT} = \frac{PI\ fluorescence\ (counts)_{final}}{Calcein\ AM\ fluorescence\ (counts)_{initial}} \quad (9)$$

To quantify the effectiveness of the 2-photon PDT, we took the ratio of the PI signal after PDT to the average PI background before PDT for each sample. We also defined statistically significant cell-death as PI fluorescence after PDT being 2 standard deviations above the PI fluorescence before PDT.

Statistical analysis

Statistical significance was determined using a two-tailed two sample t-test and expressed as (* $P < 0.05$), (** $P < 0.01$), (*** $P < 0.001$), and ns (no significance). Where relevant, the data are expressed as a mean +/- the standard deviation.

SECTION S2: ADDITIONAL DISCUSSION

Nanosystem assemblies:

Our size data suggests that modest 8-arm-PEG NP assembly occurs upon Ce6 conjugation (Table 1). This assembly is also observed in the 8-arm PEG-Ce6-dMIBG and dBG samples (and variation in particle size is significant in the TEM image of the dMIBG conjugate, Figure S11), but to a somewhat lesser extent as compared to the 8-arm PEG-Ce6 (Table 1). This suggests that the MAL-PEG-dMIBG and the MAL-PEG-dBG conjugation may interrupt the assembly of the NPs. To further evaluate the extent of the assembly, GPC characterization was applied where despite a larger 'base' size NP from the 8-arm-peg-dMIBG/dBG (which was expected), 8-arm-peg-Ce6 showed the largest tail, indicating greatest assembly (Figure S12).

ROS values:

We observed that *free* Ce6 is a more efficient ROS producer (63 ± 8 %) than TMPyP (14 ± 4 %), a popular PS with TPA properties, which has a previously recorded ROS efficacy of 18 % at 400 nm,[14, 18,19] but less than RB (75%) (Table 2). However, once Ce6 is conjugated to the 8-arm PEG nanostructure, the ROS efficacy increases almost 1.5 times (Table 1). *Free* Ce6 is known to aggregate,[20] which can induce self-quenching and, thus, limit the ROS efficacy of the PS.[21]

Since conjugating the Ce6 to 8-arm PEG effectively makes the rate of Ce6 aggregation/precipitation negligible, ROS efficacy would hence increase. It was indeed found that the ROS efficacy of the Ce6 attached to the 8-arm PEG increased to 94 ± 0.16%. Interestingly, it was also found that the presence of the dMIBG/dBG molecules attached to the complex reduces the ROS efficacy to 63 ± 4% and 49 ± 16%,

respectively, becoming more comparable to the *free* Ce6 ROS efficacy. It was previously observed that when Ce6 was encapsulated inside a polyacrylamide (PAAm) NP the ROS production was about 1.5x lower than when the Ce6 was more accessible.[4] The attachment of the long MAL-PEG chain may decrease the contact between the Ce6 and the solvent environment, influencing the ROS efficacy.

The 8-arm PEG-Ce6-dMIBG nanosystem shows a larger average ROS efficacy than that of the 8-arm PEG-Ce6-dBG. These results could be attributed to the presence of the iodine atom on the dMIBG structure due to an *external heavy atom effect*.[22] Such effect enhances the intersystem crossing from the singlet to the triplet transition, as observed in the presence of heavy atoms such as Cl, Br and especially I.[22] This is significant as it suggests that the dMIBG, with its iodine atom, enhances ROS efficacy. Additional in-depth ROS efficacy studies would need to be carried out to determine the exact ROS production *in vitro* and *in vivo*, but these *ex vitro* results are suitable to continue the relative efficacy comparison between nanosystems.

SECTION S3: SUPPLEMENTARY FIGURES

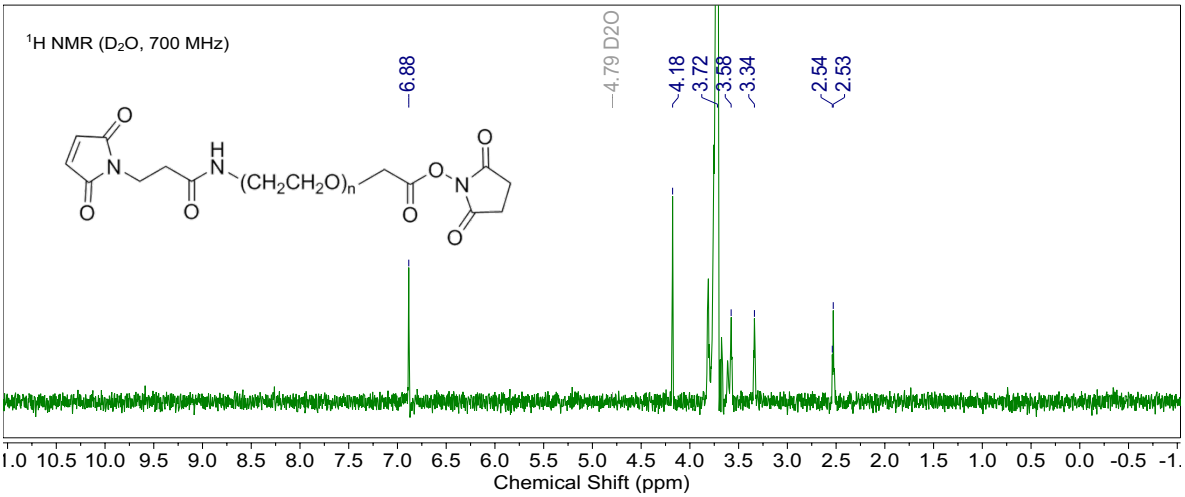

Figure S1. ^{1}H NMR of maleimide-PEG-succinimidyl carboxymethyl ester in D_2O verifies the presence of the maleimide (6.88 ppm) and succinimidyl carboxymethyl ester (2.53 ppm) pendant groups attached to the long PEG chain (3.72 and 3.76 ppm).

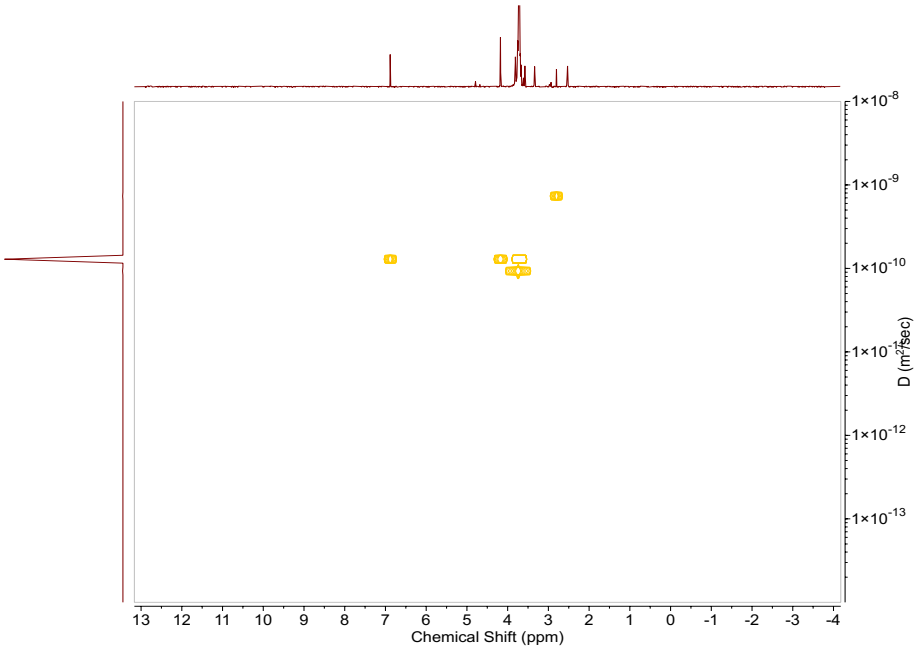

Figure S2. ^{1}H DOSY spectrum in D_2O of MAL-PEG-SCM shows although there appears to be another other compound, due to the long PEG chain it can reasonably inferred that the difference could be due to the flexible chain. Otherwise there appears to be no other significant PEG compounds in the sample illustrating the purity of the precursor.

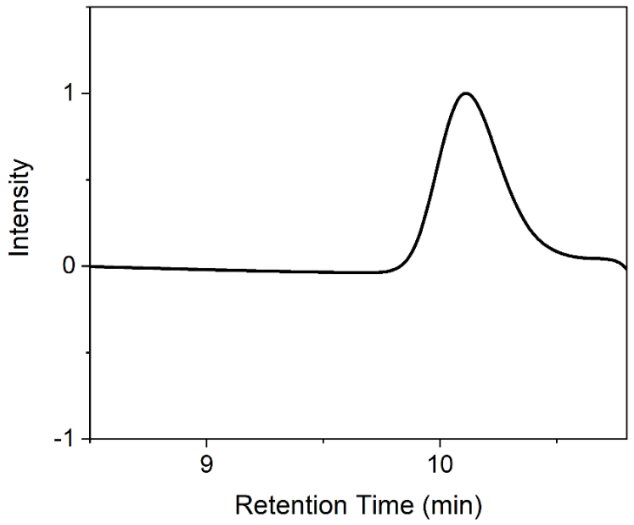

Figure S3. GPC LC (liquid chromatograph) of MAL-PEG-SCM in THF at 1 mg/mL. The number average molecular weight (M_n), weight average molecular weight (M_w), and polydispersity index (PDI) were determined to be 2.04×10^3 g/mol, 2.30×10^3 g/mol, and 1.13 respectively. This is comparable to the commercially reported 2.35×10^3 g/mol averaged MW by MALDI.

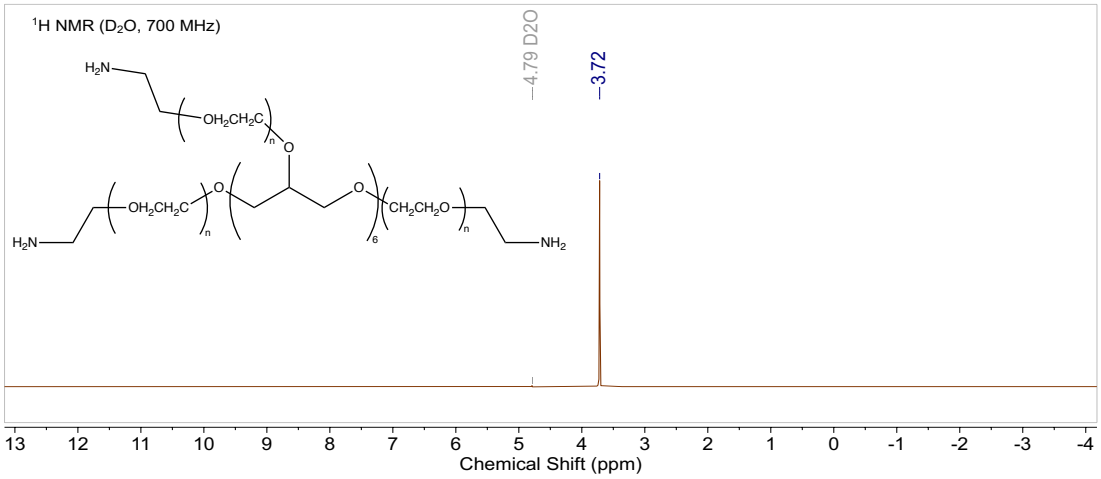

Figure S4. ^{1}H NMR of 8-arm PEG-NH_2 in D_2O (4.8 ppm) confirms that only the PEG peak is present at 3.70 ppm.

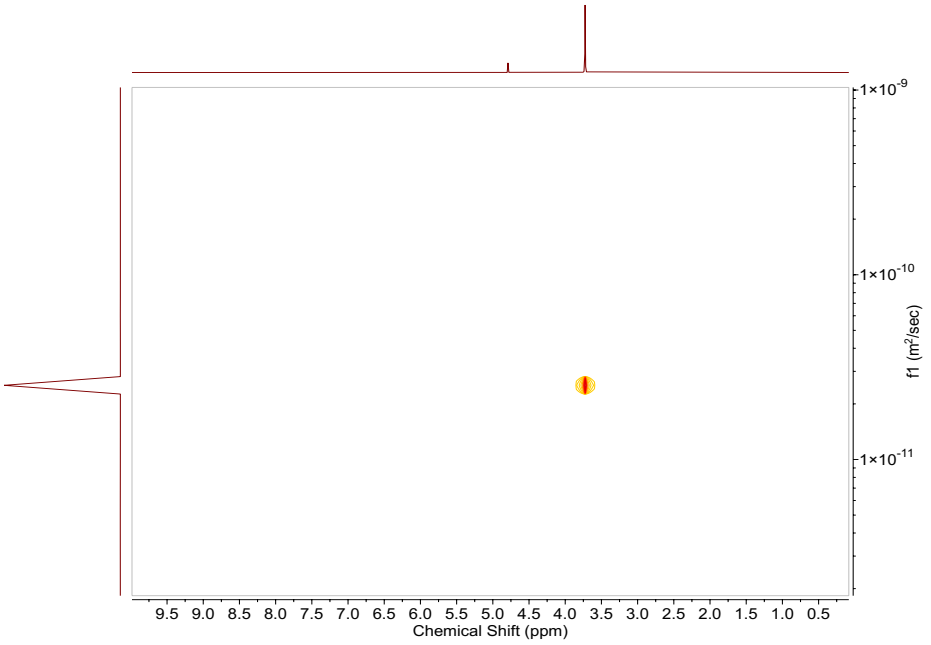

Figure S5. ^{1}H DOSY in D_2O of 8-arm PEG-NH_2 verifies that the precursor only contains PEG components and there is no presence of any other compounds. The peak at 4.8 ppm at the top of the plot is the D_2O signal.

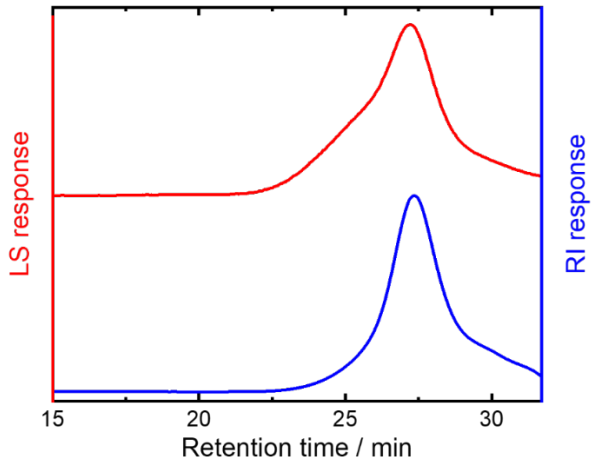

Figure S6. GPC light scattering (LS) and refractive index (RI) response for 8-arm PEG-NH_2 at 5 mg/mL. The M_n, M_w, and PDI were determined as 4.25×10^4 g/mol, 4.98×10^4 g/mol, and 1.17, respectively. This is comparable to the commercially reported 4.06×10^4 g/mol averaged MW by MALDI.

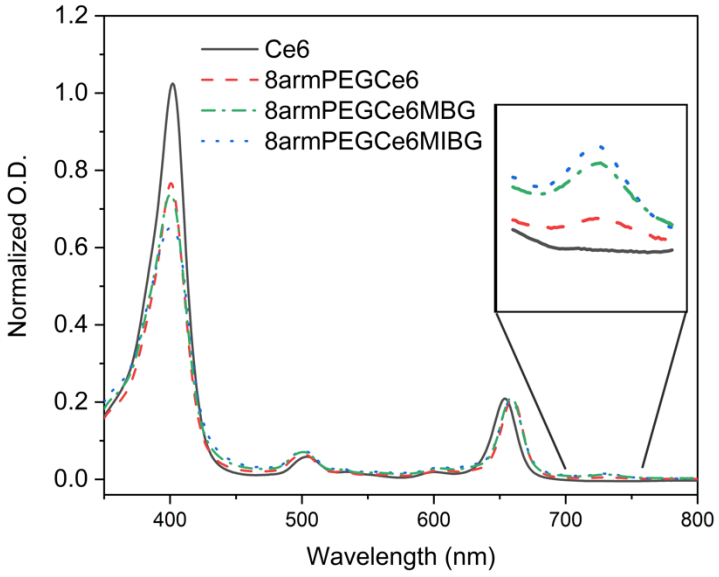

Figure S7. Uv-Vis spectra of Ce6, 8-arm PEG-Ce6, 8-arm PEG-Ce6-dMIBG, and 8-arm PEG-Ce6-dBG in 1X PBS.

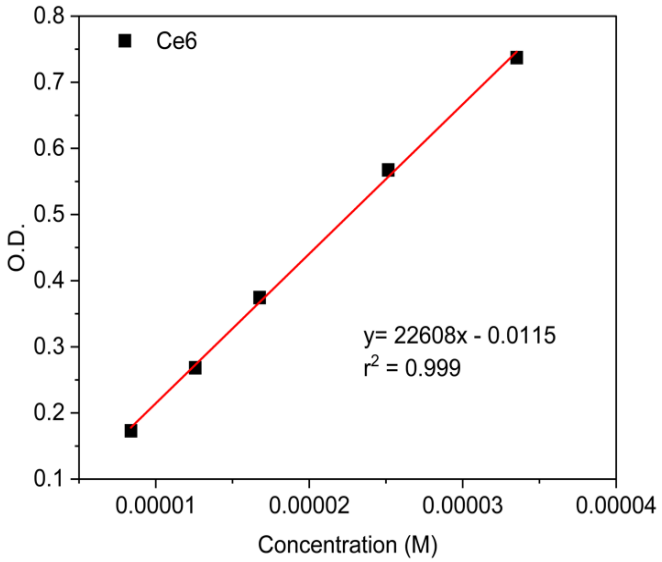

Figure S8. Ce6 calibration curve in 1X phosphate buffer saline solution (PBS) at 660 nm.

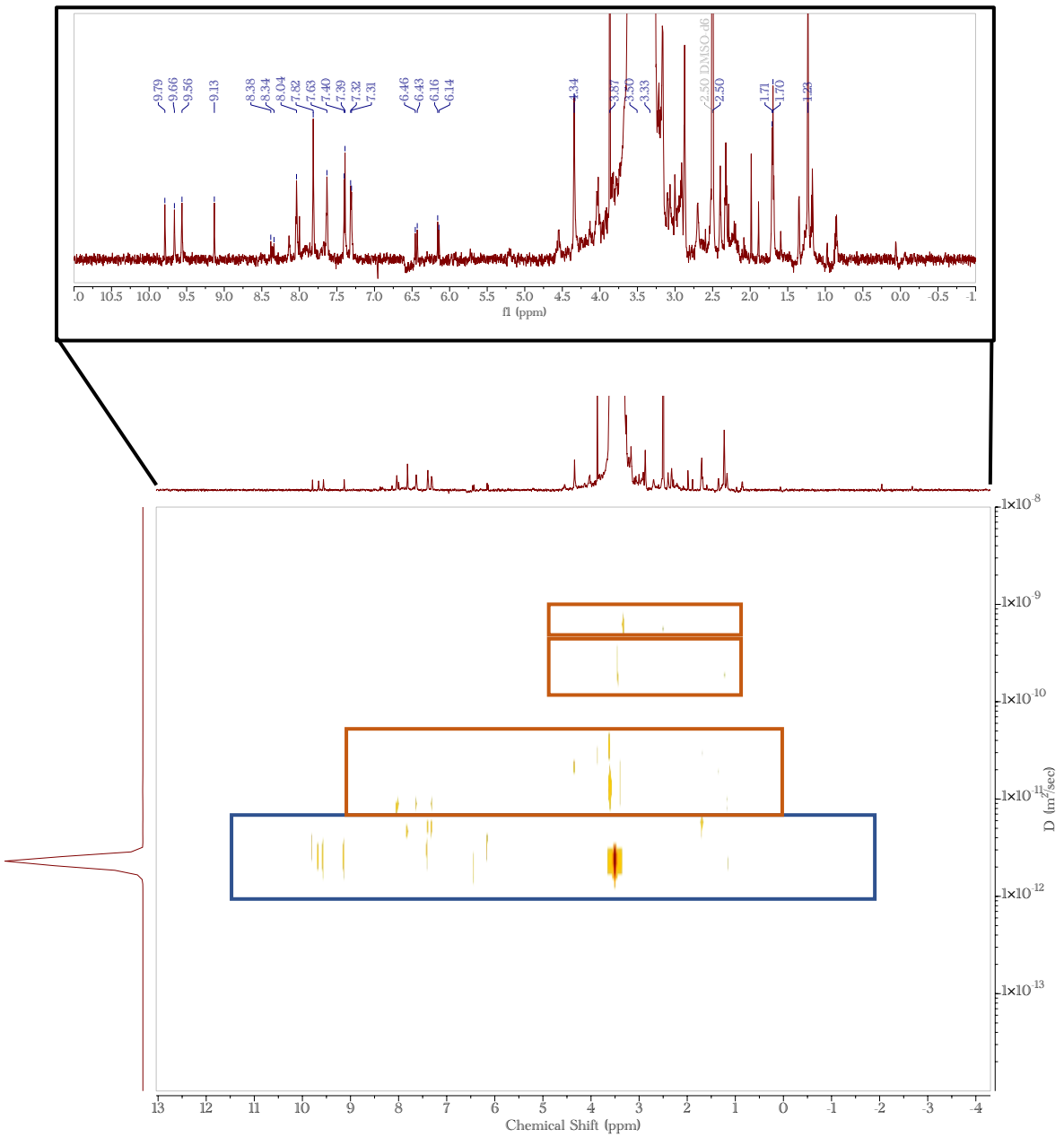

Figure S9. Diffusion ^{1}H NMR in $DMSO_{d6}$ of 8-arm PEG-Ce6-dMIBG peaks labeled (top) and verification that the dMIBG and Ce6 were successfully conjugated (blue box). Other features indicate some variation of conjugation success (orange boxes). Significant Ce6 peaks are 8.34, 6.44, 6.14, and 1.7 ppm. Significant dMIBG peaks are 7.8, 7.31-7.4, 4.34 ppm. The main PEG peak is at 3.50 ppm.

Table S1a. Characteristic peaks of Ce6 and dMIBG from Figure S9 spectrum.

Ce6 peaks			dMIBG peaks		
N -nuclei	ppm	integration	N	ppm	integration
6	1.7	7.2	2	4.34	4.54
1	6.14	1.01	2	7.4-7.31	6.08
1	6.44	1	1	7.82	3.08
1	8.34	0.9			

Table S1b. Averaged molar ratios using the characteristic peaks of dMIBG and Ce6 (n=4)

	4.34 ppm peak	7.4-7.31 ppm peak	7.82 ppm peak	Total average
Molar ratio dMIBG to Ce6	2.23 ± 0.26	2.99 ± 0.35	3.03 ± 0.35	2.75 ± 0.45
Molar ratio of dMIBG to 8-arm PEG-Ce6	4.47 ± 0.52	5.98 ± 0.35	6.06 ± 0.70	5.50 ± 0.90

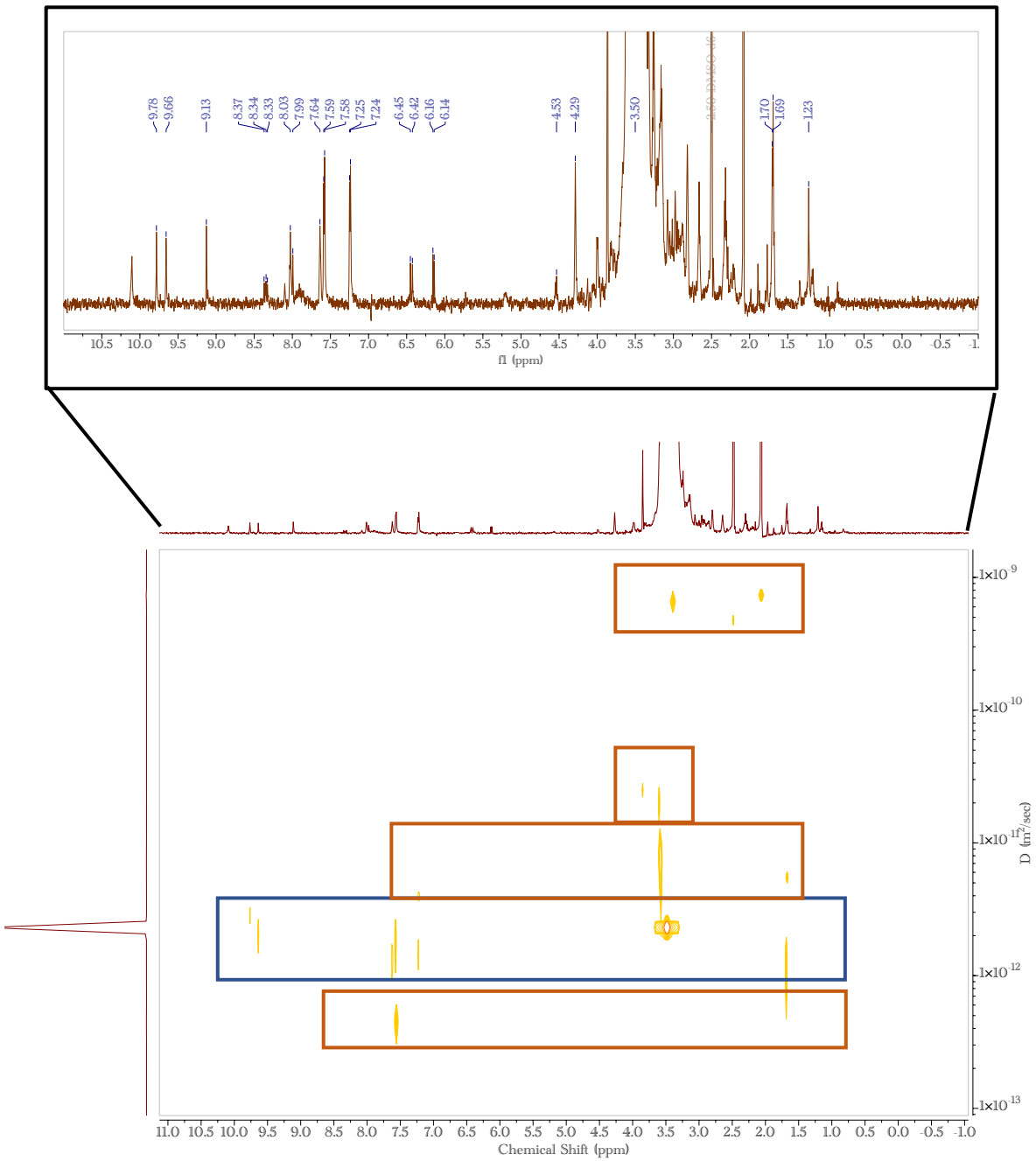

Figure S10. Diffusion ^{1}H NMR in $DMSO_{d6}$ of 8-arm PEG-Ce6-dBG peaks labeled (top) and verification that the dBG and Ce6 were successfully conjugated (blue box). Other features indicate some variation of conjugation success (orange boxes). Significant Ce6 peaks are 8.34, 6.43, 6.14, and 1.7 ppm. Significant dBG peaks are 7.64-58, 7.24, and 4.30 ppm. The main PEG peak is at 3.50 ppm.

Table S2a. Characteristic peaks of Ce6 and dBG from Figure S10 spectrum.

Ce6 peaks			dBG peaks		
N -nuclei	ppm	integration	N	ppm	integration
6	1.7	6.28	2	4.30	2.40
1	6.14	0.90	2	7.24	3.15
1	6.43	1	2	7.64- 7.58	4.42
1	8.34	0.93			

Table S2b. Averaged molar ratios using the characteristic peaks of dBG and Ce6 (n=4)

	7.64-7.58 ppm peak	7.24 ppm peak	4.30 ppm peak	Total average
Molar ratio dBG to Ce6	1.53 ± 0.1	1.63 ± 0.11	1.24 ± 0.08	1.47 ± 0.2
Molar ratio of dBG to 8-arm PEG-Ce6	2.76 ± 0.19	3.62 ± 0.25	3.39 ± 0.23	3.26 ± 0.45

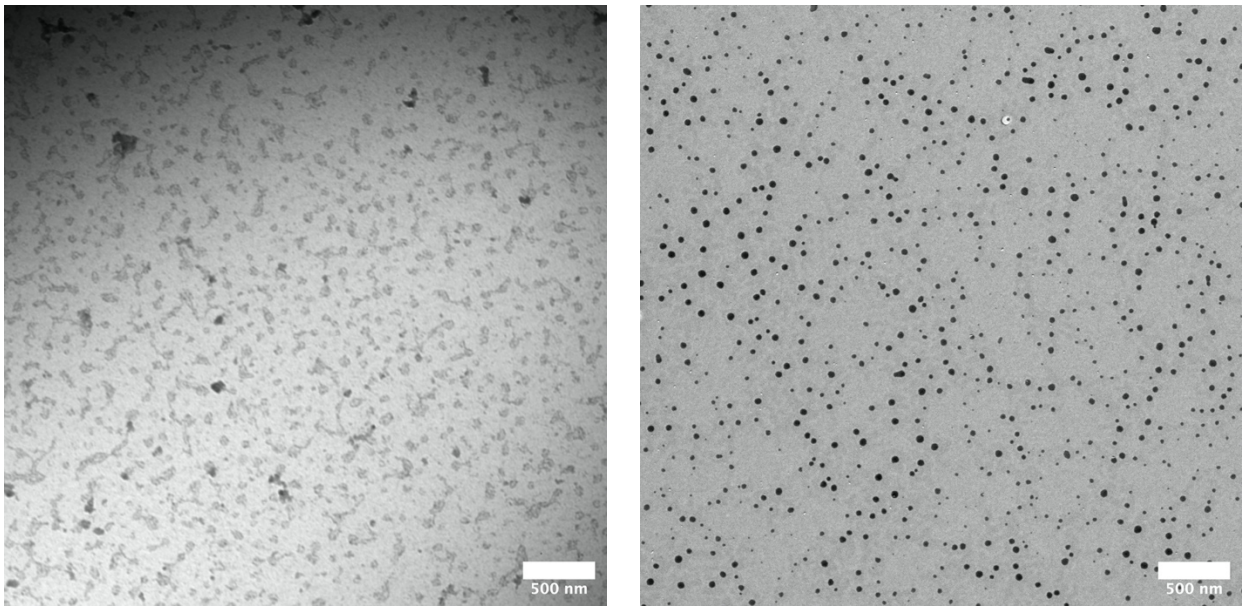

Figure S11. TEM of 8-arm PEG Ce6-dBG (left) and 8-arm PEG Ce6-dMIBG (right) showing difference in contrast observed.

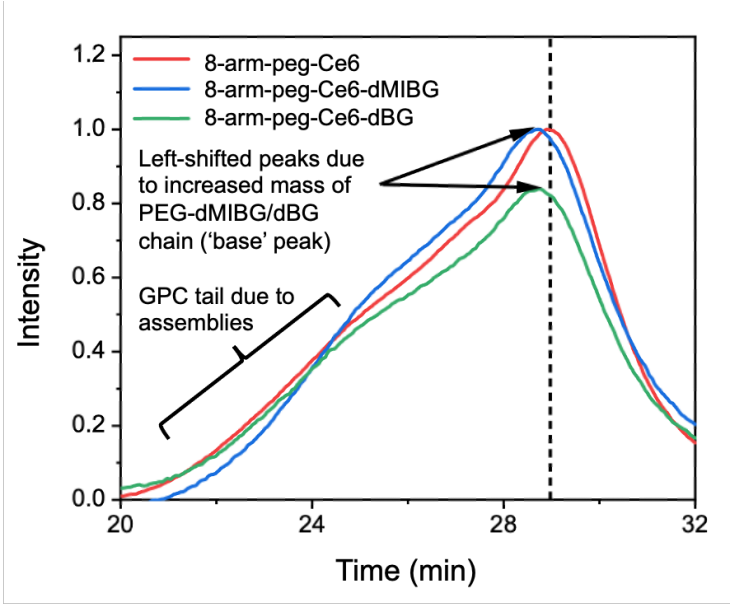

Figure S12. GPC UV-Vis signal of 8-arm PEG nanosystems at 1.0 mg/mL. Earlier elution time results correspond to a larger molecular weight (8-arm-PEG had no signal due to lack of optical fluorophore and is therefore not shown).

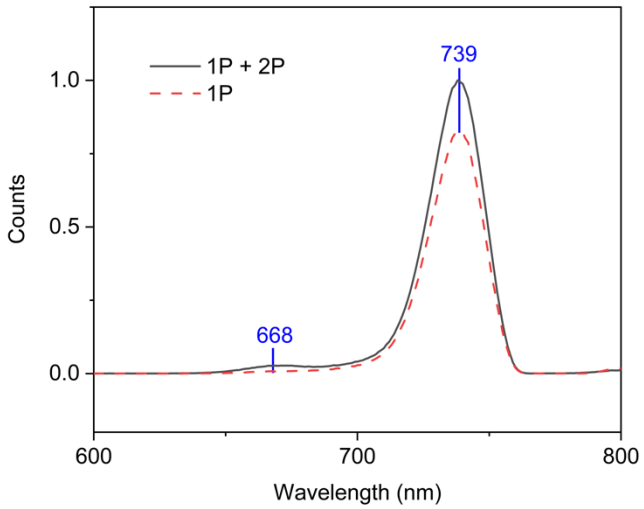

Figure S13. 2-photon fluorescence (counts normalized to 1P and 2P peak at 739 nm) of 8-arm PEG-Ce6-dMIBG using a 1P (un-pulsed laser) and 1 + 2P (pulsed laser) tuned to 800 nm (at 0.383 W power).

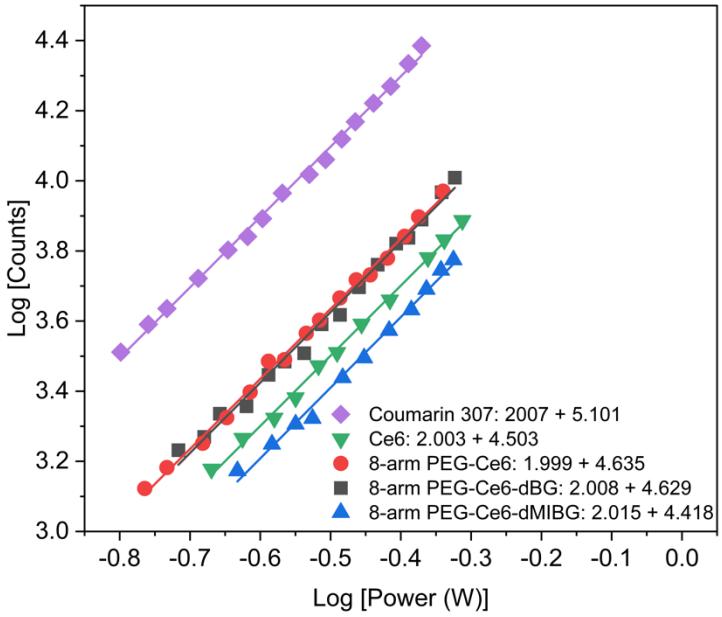

Figure S14. 2-photon log[counts] vs. log [Power] graph of Coumarin 307 at 506 nm, Ce6, 8-arm PEG-Ce6, 8-arm PEG-Ce6-dMIBG, and 8-arm PEG-Ce6-dBG at 668 nm all used to calculate the 2-photon cross sections.

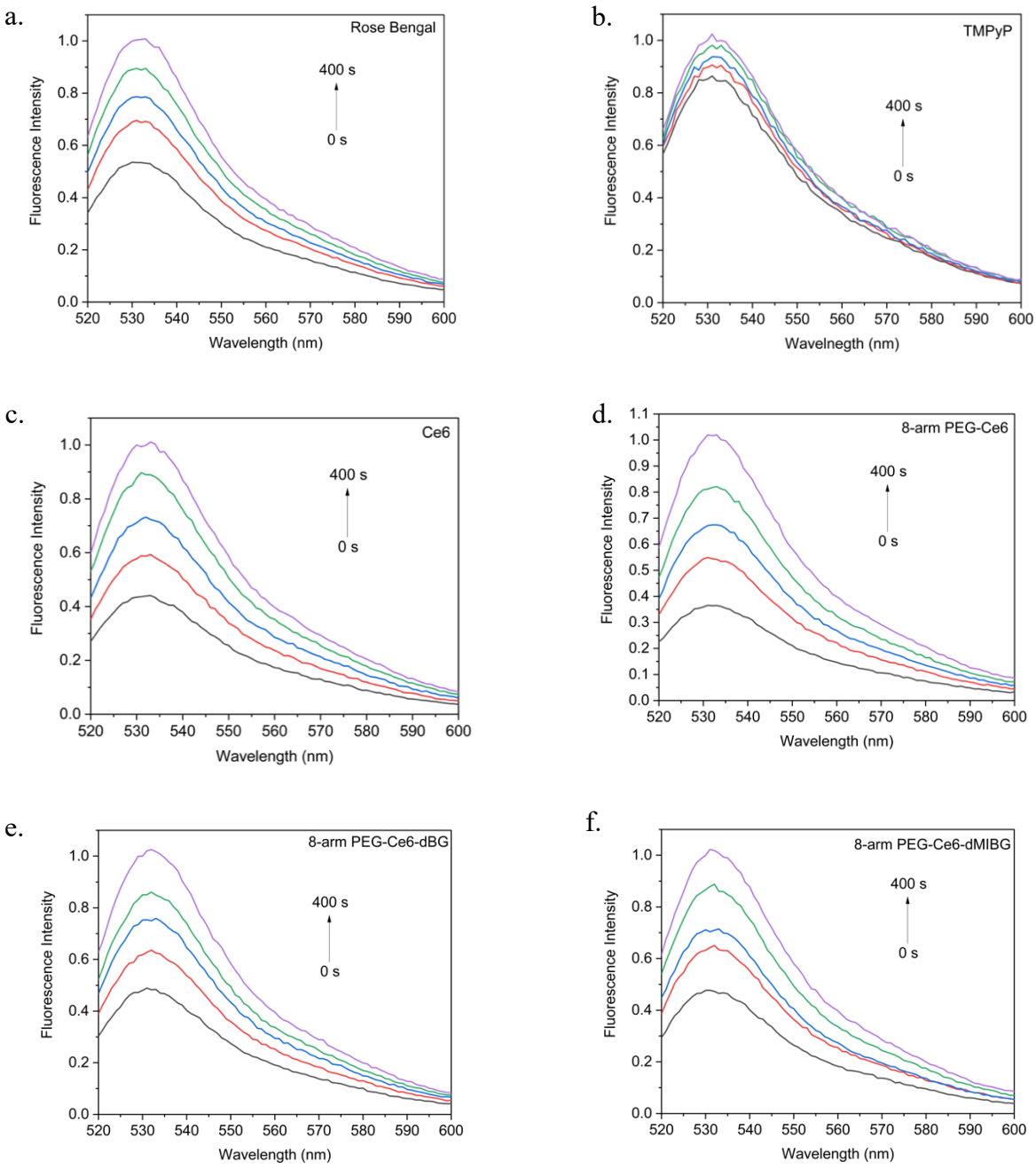

Figure S15. SOSG-EP emission spectra change at 530 nm after 100 s irradiations for a total of 400 s. (a) RB (b) TMPyP (c) Ce6 (d) 8-arm PEG-Ce6 (e) 8-arm PEG-Ce6-dMIBG (f) 8-arm PEG-Ce6-dBG.

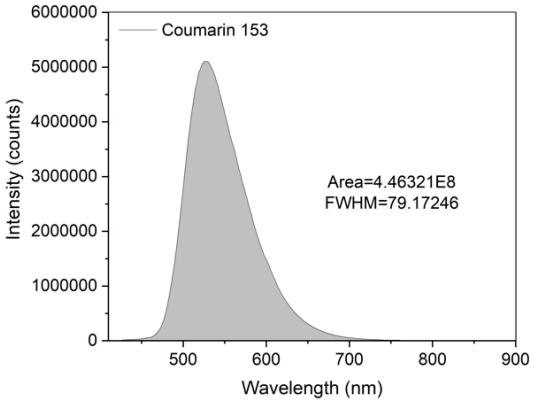

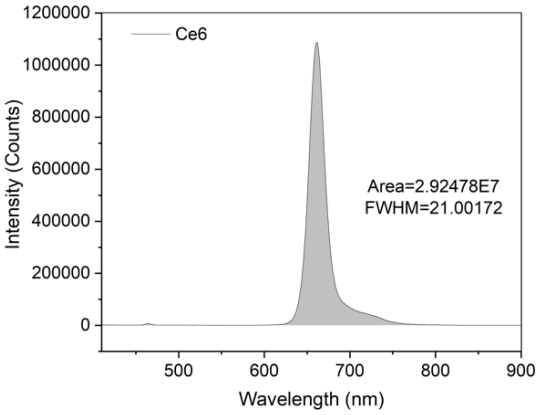

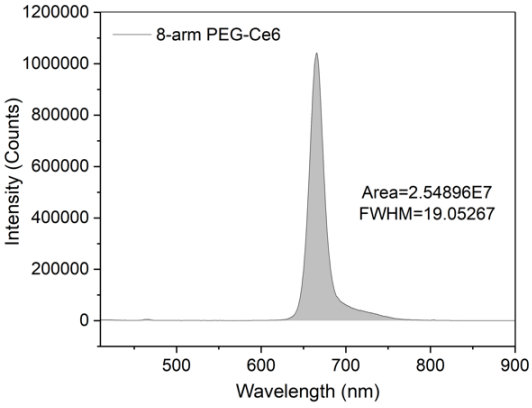

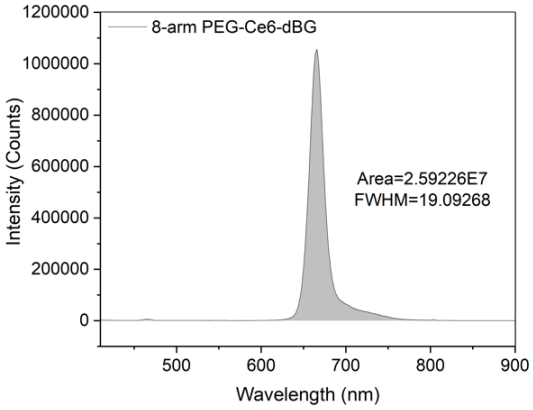

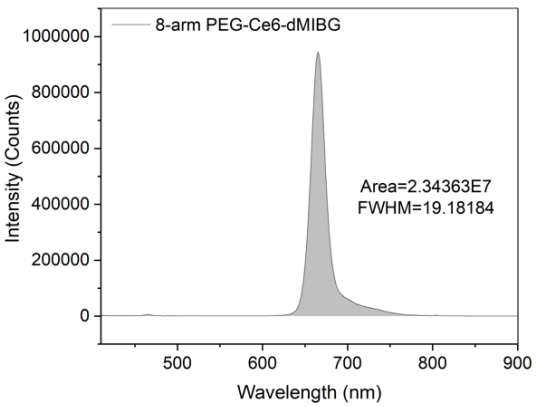

Compound	Quantum Yield
Ce6	3.22%
8-arm PEG-Ce6	2.98%
8-arm PEG-Ce6-dBG	2.89%
8-arm PEG-Ce6-dMIBG	2.61%

Figure S16. Integrated fluorescence emission of Coumarin 153 (EtOH), Ce6 (1X PBS), 8-arm PEG-Ce6 (1X PBS), 8-arm PEG-Ce6-dBG (1X PBS), and 8-arm PEG-Ce6-dMIBG (1X PBS). Excitation: 400 nm Emission: 410-900 nm. Using the area and the literature quantum yield for Coumarin 153, the fluorescence quantum yields were determine and are provided in the inlet.

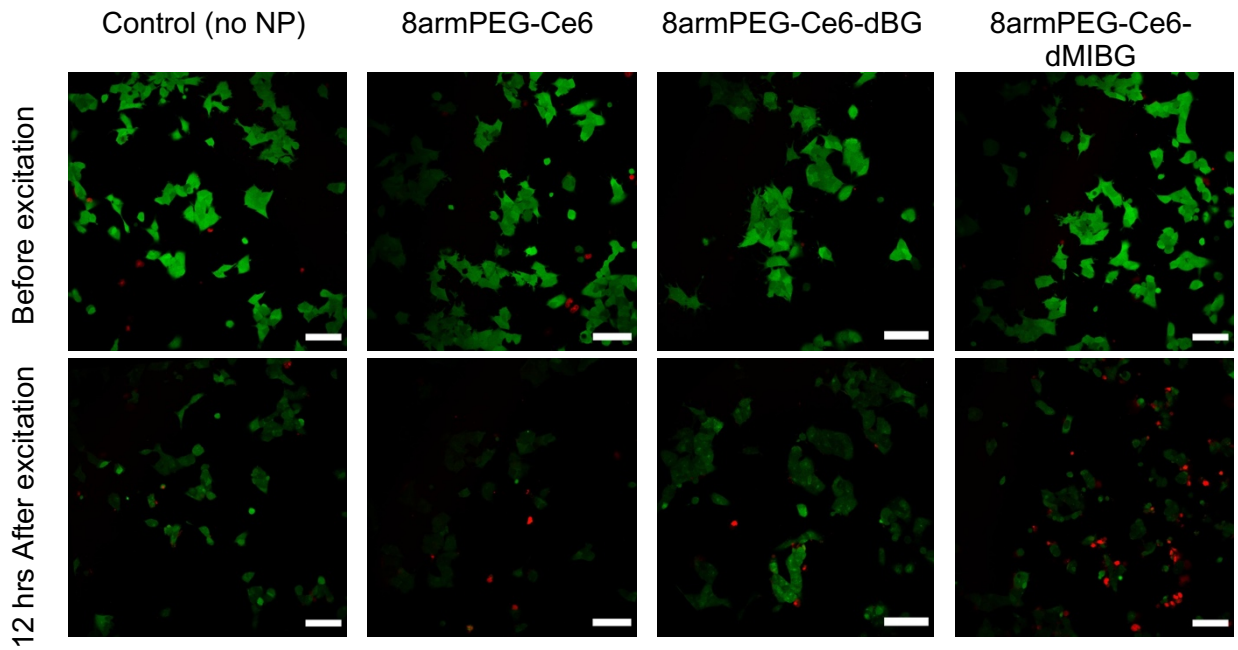

Figure S17. PDT images ('trial 1') of SK-N-BE(2)C neuroblastoma cells with control (no nanoparticle) as well as when incubated with 1 μM of 8armPEG-Ce6, 8armPEG-Ce6-dBG, and 8armPEG-Ce6-dMIBG. Samples were co-stained with Calcein AM and propidium iodide (PI) to indicate viability. Scale bar is 100 μm.

Table S3. Quantitative analysis of 2p-PDT images from Fig. S17.

Sample	Ratio ($Red/Green_{initial}$)	Mag. Increase	Statically Significant?
Background (before PDT; *n* = 4)	0.006 (± 0.005)	-	-
After PDT			
Control	0.004 ± 0.001	0.6 ± 0.2	No
8-arm PEG-Ce6	0.011 ± 0.002	1.7 ± 0.4	No
8-arm PEG-Ce6-dBG	0.006 ± 0.002	1.1 ± 0.4	No
8-arm PEG-Ce6-dMIBG	0.037 ± 0.016	6.1 ± 2.7 (*6.4 ± 2.8 STDEVs*)	Yes

All analysis was done *via* ImageJ/Fiji image analysis and Excel for calculations (more details in Section S1). "Mag. Increase" refers to the increase of red relative of the final image to the averaged relative red before excitation (background PI fluorescence; *n=4*). Statistically significant is defined as 2 standard deviations above the background mean or >95 percentile.

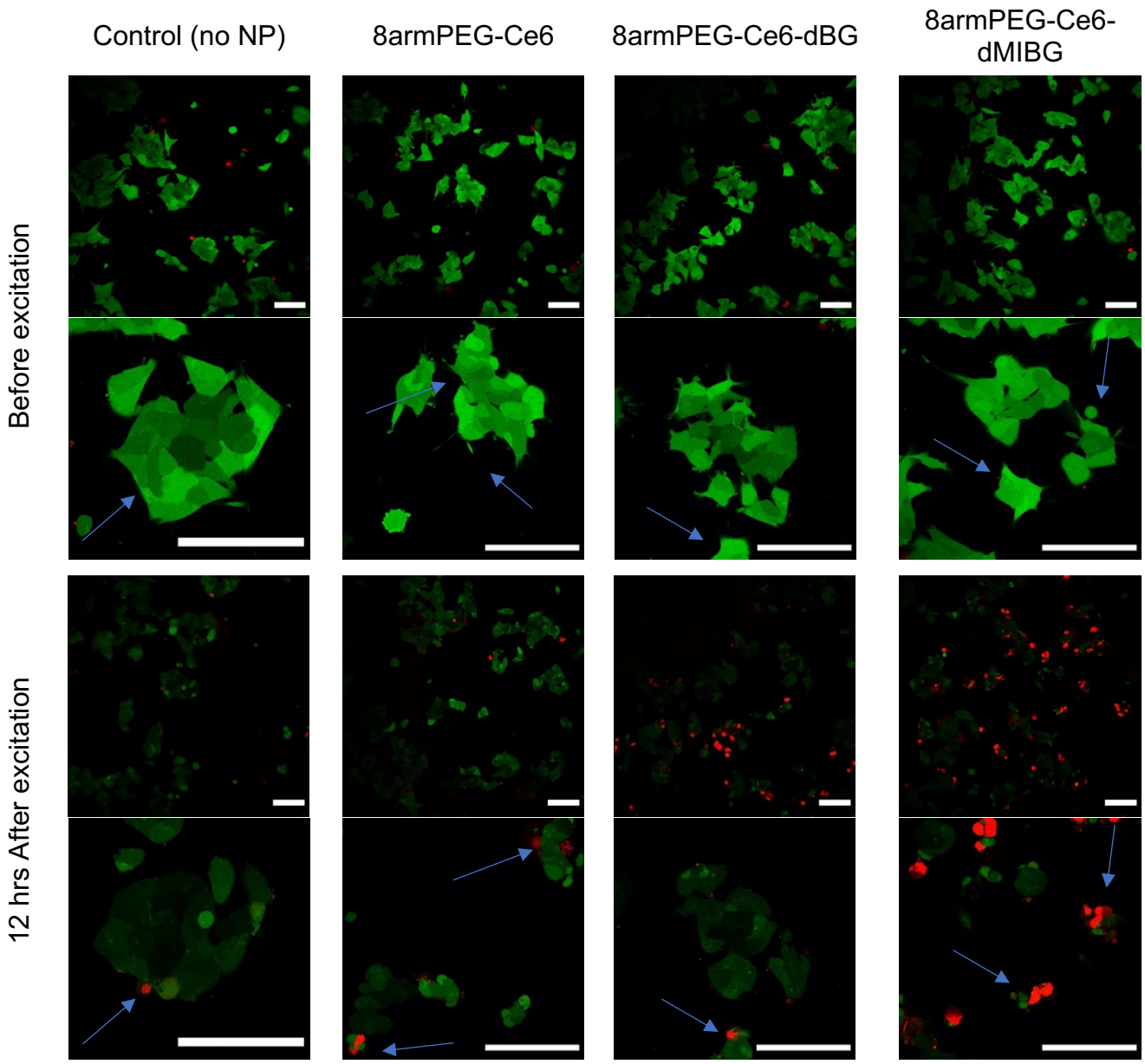

Figure S18. PDT images ('trial 2') of SK-N-BE(2)C neuroblastoma cells with control (no nanoparticle) as well as when incubated with 1 μM of 8armPEG-Ce6, 8armPEG-Ce6-dBG, and 8armPEG-Ce6-dMIBG. Samples were co-stained with Calcein AM and propidium iodide (PI) to indicate viability. Scale bar is 100 μm for the full plate image and 200 μm for the zoomed in image.

Table S4. Quantitative analysis of 2p-PDT images from Fig. S18 (zoomed-out images).

Sample	Ratio ($Red/Green_{initial}$)	Mag. Increase	Statically Significant?
Background (before PDT; *n* = 4)	0.007 (± 0.008)	-	-
After PDT			
Control	0.006 ± 0.002	0.8 ± 0.3	No
8-arm PEG-Ce6	0.020 ± 0.005	2.8 ± 0.7	No
8-arm PEG-Ce6-dBG	0.110 ± 0.020	15.3 ± 2.7 (13.1 ± *2.3 STDEVs*)	Yes
8-arm PEG-Ce6-dMIBG	0.119 ± 0.009	16.6 ± 1.3 (14.2 ± *1.1 STDEVs*)	Yes

All analysis was done *via* ImageJ/Fiji image analysis and Excel for calculations (more details in Section S1). "Mag. Increase" refers to the increase of red relative of the final image to the averaged relative red before excitation (background PI fluorescence; *n=4*). Statistically significant is defined as 2 standard deviations above the background mean or >95 percentile.

References

1. N. S. Potter, A. McLean, E. C. Bornowski, T. Hopkins, J. Luo, J. P . Wolfe, W. Qian, R. Kopelman, *ACS Mater. Lett*., 2023, 5, 2971 – 2977.
2. U. M. R. Avula, H. K. Yoon, C. H. Lee, K. Kaur, R. J. Ramirex, Y. Takemoto, S. R. Ennis, F. Morady, T. Herron, O. Berenfeld, R. Kopleman and J. Kalifa, *Sci. Transl. Med*., 2015, 7, 20–37.
3. B. Yu, Y. Yang, Q. Liu, A. Zhan, Y. Yang and H. Liu, *Pharmaceutics*, 2020, 12, 329–342.
4. T. Hopkins, S. D. Swanson, J. D. Hoff, N. Potter, R. Ukani R. Kopelman, *ACS Appl. Bio. Mater*., 2018, 1, 1094–1101.
5. K. Choi; S. Myoung, Y. Seo, S. Ahn, *Magnetochemistry*, 2021, 7, 15.
6. P. Groves, *Polym. Chem*., 2017, 8, 6700-6708.
7. K. Gu, J. Onorato, S. S. Xiao, C. Luscombe, Y.-L. Loo, *Chem. Mater.,* 2018, *30*, 570-576.
8. H. Hasse, H.-P. Kany, R. Tintinger, G. Maurer, *Macromolecules,* 1995, *28*, 3540-3552.
9. M. Brouwer *Pure Appl. Chem.,* 2011, *83*, 2213-2228.
10. K. Rurack and M. Spieles, *Anal. Chem.,* 2011, *83*, 1232-1242.
11. F. Wilkinson, W.P. Helman, A. B. Ross, *J. Phys. Chem. Ref. Data* 1993, *22*, 113-262
12. H. Lin, Y. Shen, D. Chen, L. Lin, B. C. Wilson, B. Li, S. Xie, *J. Fluoresce.,* 2013, 23, 41-47.
13. A. McLean, R. Wang, Y. Huo, A. Cooke, T. Hopkins, N. Potter, J. Isaac, J. Haidar, R. Jin, R. Kopelman, *ACS Appl. Nano Mater.* 2020, *3*, 1420-1430.
14. C. Xu and W. W. Webb, *J. Opt. Soc. Am. B* 1996, *3*, 481-491.
15. J. Schmitt, V. Heitz, A. Sour, F. Bolze, H. Ftouni, J.F. Nicoud, L. Flamigni, B. Ventura. Angew. *Chem. Int. Ed.* 2015, 54, 169–173.
16. J. Schmitt, V. Heitz, A. Sour, F. Bolze, P. Kessler, L. Flamigni, B. Ventura, C.S. Bonnet, E. Tóth, *A Chem-Eur. J.* 2016, 22, 2775–2786.
17. F.L Miles, J.E. Lynch, R.A. Sikes, *J. Biol. Methods*. 2015, 2, e29.
18. D. Gao, R. R. Agayan, H. Xu, M. A. Philbert and R. Kopelman, *Nano Lett.*, 2006, 6, 2383–2386.
19. Y. Shen, A. J. Shuhendler, D. Ye, J.-J. Xua and H.-Y. Chen, *Chem. Soc.*

Rev., 2016, 45, 6725–6741.

20. P. Li, G. Zhou, X. Zhu, G. Li, P. Yan, L. Shen, Q. Xu and M. R. Hamblin, *Photodiagnosis. Photodyn. Ther.*, 2012, 9, 76–82.
21. D. B. Tada and M. S. Baptista, *Front. Chem.*, 2015, 3, 33.
22. C. M. Marian, *Annu. Rev. Phys. Chem.*, 2021, 72, 617–640.